

available at www.sciencedirect.comwww.elsevier.com/locate/brainres

**BRAIN
RESEARCH**

Research Report

Spatiotemporospectral characteristics of scalp ictal EEG in mesial temporal lobe epilepsy with hippocampal sclerosis

Ki-Young Jung^{a,*}, Joong-Koo Kang^b, Ji Hyun Kim^c, Chang-Hwan Im^d,
Kyung Hwan Kim^d, Hyun-Kyo Jung^e

^aDepartment of Neurology, Korea University Medical Center, Korea University College of Medicine, #126-1, Anam-Dong 5Ga, Seongbuk-Gu, Seoul 136-705, Republic of Korea

^bDepartment of Neurology, Ulsan University College of Medicine, Seoul, Republic of Korea

^cDepartment of Neurology, Korea University Medical Center Guro Hospital, Korea University College of Medicine, Seoul, Republic of Korea

^dDepartment of Biomedical Engineering, Yonsei University, Wonju, Republic of Korea

^eSchool of Electrical Engineering, Seoul National University, Seoul, Republic of Korea

ARTICLE INFO

Article history:

Accepted 23 June 2009

Available online 27 June 2009

Keywords:

Temporal lobe epilepsy

Hippocampal sclerosis

Ictal EEG

Independent component analysis

Dipole source localization

Spatiotemporal propagation

ABSTRACT

The aim of present study was to identify the common propagation pattern of ictal discharges in mesial temporal lobe epilepsy (TLE). Pre-surgical ictal scalp EEG recordings were collected from patients with TLE associated with hippocampal sclerosis. Two types of ictal onset patterns were identified based on spatial and spectral characteristics of initial ictal discharge waveforms: (a) a sustained regular 5- to 9-Hz rhythm with a restricted temporal or subtemporal distribution (type 1); and (b) an irregular 2- to 5-Hz rhythm with a widespread distribution (type 2). Scalp EEG data were decomposed into temporally independent, spatially fixed component by independent component analysis. The identified source activities corresponding to ictal discharges from each seizure were localized by dipole source localization, and dipole sources with similar spatial locations were clustered. To identify the sequence of propagation among component clusters during the progress of seizures, event-related spectral perturbation by wavelet transform was used. Fifty-five seizures (22 seizures in four Type 1 patients and 33 seizures in eight Type 2 patients) in 12 patients were analyzed. Ictal discharges associated with type 1 seizures arose from both the anterior temporal region and basal ganglia, and then spread into medial frontal region. The dominant frequency of ictal rhythm was in the theta range and remained relatively constant until the middle portion of seizures. Type 2 seizures developed bilaterally or predominantly in the ipsilateral medial temporal region, followed by the medial frontal region and basal ganglia. The dominant frequency of ictal activity at the onset of seizure was in the delta range. However, rhythmic theta activities with decreasing tendency ensued rapidly after seizure onset. These findings suggest that TLE associated with hippocampal sclerosis may have preferential propagating patterns according to the type of the ictal onset pattern.

© 2009 Elsevier B.V. All rights reserved.

* Corresponding author. Fax: +82 2 925 2472.

E-mail addresses: jungky@korea.ac.kr, jungky10@gmail.com (K.-Y. Jung).

1. Introduction

Scalp ictal EEG reveals common rhythmic sinusoidal activities or repetitive epileptiform discharges that evolve in frequency, field, or morphology. Initial seizure patterns in mesial temporal lobe epilepsy (TLE) consist of rhythmic activities in the delta, theta, or alpha ranges, and are regionalized over the ipsilateral temporal area or lateralized to the ipsilateral hemisphere (Ebner and Hoppe, 1995). Ebersole and Pacia reported two distinct ictal onset patterns (IOPs) on scalp EEGs in mesial TLE: a temporal 5- to 9-Hz rhythmic discharge (type 1) and an irregular widely spread 2- to 5-Hz discharge (type 2) (Ebersole and Pacia, 1996; Pacia and Ebersole, 1997). Recently, we reported that ictal hyperperfusion patterns in TLE with hippocampal sclerosis (HS) were closely correlated with the IOPs of Ebersole and Pacia, based on ictal SPECT study (Kim et al., 2007). In particular, we found that the type 1 pattern showed hyperperfusion confined mainly to the ipsilateral temporal lobe, whereas the type 2 pattern showed widespread hyperperfusion in extratemporal structures, such as, the ipsilateral basal ganglia, brainstem, and bilateral thalamus, in addition to the ipsilateral temporal lobe. Because surgical outcome was good for both patterns, we hypothesized that IOPs might represent common preferential pathways of ictal propagation rather than an intrinsic epileptogenic region. However, we could not confirm our hypothesis because of limited temporal resolution of the ictal SPECT study (Duncan, 2002).

Scalp ictal EEG can be used for the non-invasive recording of brain electrical activities with high temporal resolution, although the poor spatial resolution of scalp EEG causes limitations when attempting to localize cerebral sources (Tao et al., 2007). A source localization method has been described that might allow intracerebral sources to be precisely localized, at least at the sublobar level by scalp EEG (Lantz et al., 2001). Such methods may allow the identification of generators of particular EEG activities, and furthermore, pathophysiological mechanisms could be deduced from the localizations of current sources. However, few ictal EEG rhythm studies have been performed since source localization methods became available, even though ictal EEG is far more important for localizing epileptic foci. This under-utilization may be because the frequencies and distributions of dominant ictal rhythms tend to change with time, and because a variety of artifacts inevitably accompany behavioral seizures.

Independent component analysis (ICA) can separate complex multi-channel data into spatially fixed and temporally independent components, which can be regarded as sources of scalp EEG, without detailed models of either the dynamics or spatial structures of the separated components (Delorme and Makeig, 2004). The mathematical idea behind ICA is to minimize mutual information among the data projections. As decomposed components produced by ICA are temporally independent and spatially fixed, each independent component has its own scalp voltage topographic distribution. Accordingly, the spatial locations of independent components could be identified by source localization using one or more dipoles. The usefulness of the source

localization of independent components based on the dipole model and current density reconstruction after ICA was recently demonstrated (Barbati et al., 2006; Jung et al., 2005; Kobayashi et al., 2001; Marco-Pallares et al., 2005).

The present study was undertaken to identify distinct propagation patterns of ictal activity in mesial temporal lobe epilepsy according to IOPs, using an ICA-based method for localizing the sources of scalp ictal EEGs. For this purpose, we extracted independent components of ictal discharges by ICA (Nam et al., 2002). We then localized the dipole sources of these selected independent components, as reported previously (Iriarte et al., 2006; Leal et al., 2006). To identify common ictal components based on similarities between their dominant spatiotemporal patterns across seizures in multiple patients, dipole sources with similar spatial locations were clustered onto a standard brain MRI template (Jung et al., 2007; Onton et al., 2005), and to define temporal relationships between component clusters, time-frequency spectral analysis was performed on each dipole cluster (Iriarte et al., 2006; Leal et al., 2006; Onton et al., 2005).

2. Results

2.1. Patient's clinical characteristics

Twenty-one patients that underwent temporal lobectomy due to unilateral HS and achieved an excellent surgical outcome were initially enrolled. Nine patients were excluded for the following reasons: two showed switching of ictal discharges to the contralateral side during seizure, two inconsistent IOPs between seizures (i.e., for cases that both IOPs were present in a patient), and five non-lateralizing ictal patterns. Of the 12 patients finally included in the study, four (left TLE/right TLE, 2/2) were classified as having type 1 pattern and eight (left TLE/right TLE, 4/4) were type 2 pattern. The demographics and clinical characteristics of the 12 patients are summarized in Table 1. No significant differences were observed between the type 1 and type 2 groups in terms of mean age at surgery or seizure onset. Patients in both groups were found to have similar frequencies and durations of seizures as determined by video-EEG monitoring and similar febrile convulsion histories.

Table 1 – Clinical characteristics of patients.

	Type 1	Type 2	P-value
No. of patients (L/R)	4 (2/2)	8 (4/4)	
Age at surgery (mean ± SD) (y)	27.5 ± 6.1	32.0 ± 9.0	0.061 ^a
Age at onset (y)	20.7 ± 12.4	18.5 ± 11.4	0.761 ^a
Epilepsy duration (y)	20.5 ± 10.1	14.7 ± 7.6	0.273 ^a
History of febrile convulsion (%)	2 (50.0)	4 (50.0)	1.000 ^b
Follow-up period (month)	65.5 ± 27.1	63.2 ± 25.4	0.753 ^a
Seizure frequency (per month)	2.3 ± 1.5	3.8 ± 3.2	0.472 ^a
Seizure duration recorded by video-EEG (s)	81.7 ± 15.3	79.1 ± 17.9	0.652 ^a

L: left mesial temporal lobe epilepsy, R: right mesial TLE.

^a Mann-Whitney U test.

^b Fisher's exact test.

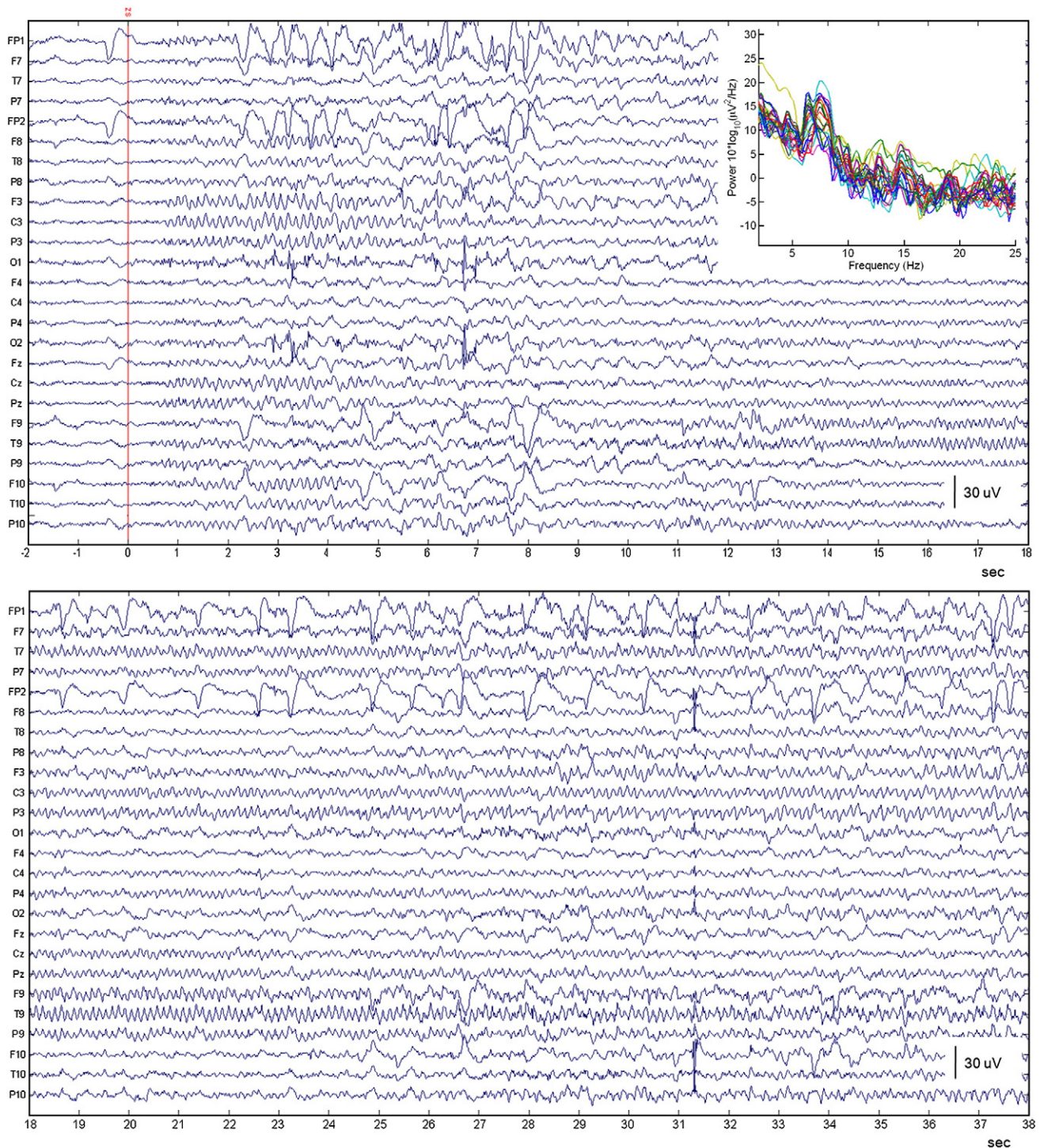


Fig. 1 – An example of an ictal scalp EEG with a type 1 ictal onset pattern (patient no. 1). The EEG displayed with common average reference. The red vertical line indicates the onset of EEG seizure. Insert is an overlay of the power spectra on the first 30 s seizure from all channels.

2.2. Seizure propagation patterns for each seizure event (level 1 analysis)

Fifty-five seizures (mean 4.2/patient \pm 2.2) were analyzed. The mean number of independent components (ICs) accounting

for ictal activity of each seizure was 3.7 \pm 1.4 (range, 2–5). Below, we describe individual seizures in two cases in detail.

Patient no. 1 was 32 year old woman who had experienced complex partial seizures for 15 years. She had a febrile seizure at two years of age. Her seizures usually started with

strange feeling and developed to motionless staring with loss of contact. Brain MRI revealed HS in the left mesial temporal lobe. Seven seizures were recorded with video-EEG monitoring during the pre-surgical evaluation. Seizure showed rhythmic theta activity arising from the left frontotemporal regions by scalp EEG (Fig. 1). Power spectral analysis on the first 30 s of these seizures showed peak

power at 6–8 Hz (insert). Accordingly, her seizures were categorized as type 1.

The time courses of ICs, corresponding scalp topographic maps, and equivalent single dipole sources are presented in Figs. 2 and 3, respectively. Five ICs were selected for seizure activities (Fig. 4), which accounted for 28.3% of total variances during the 30 s post seizure onset. The locations of the single

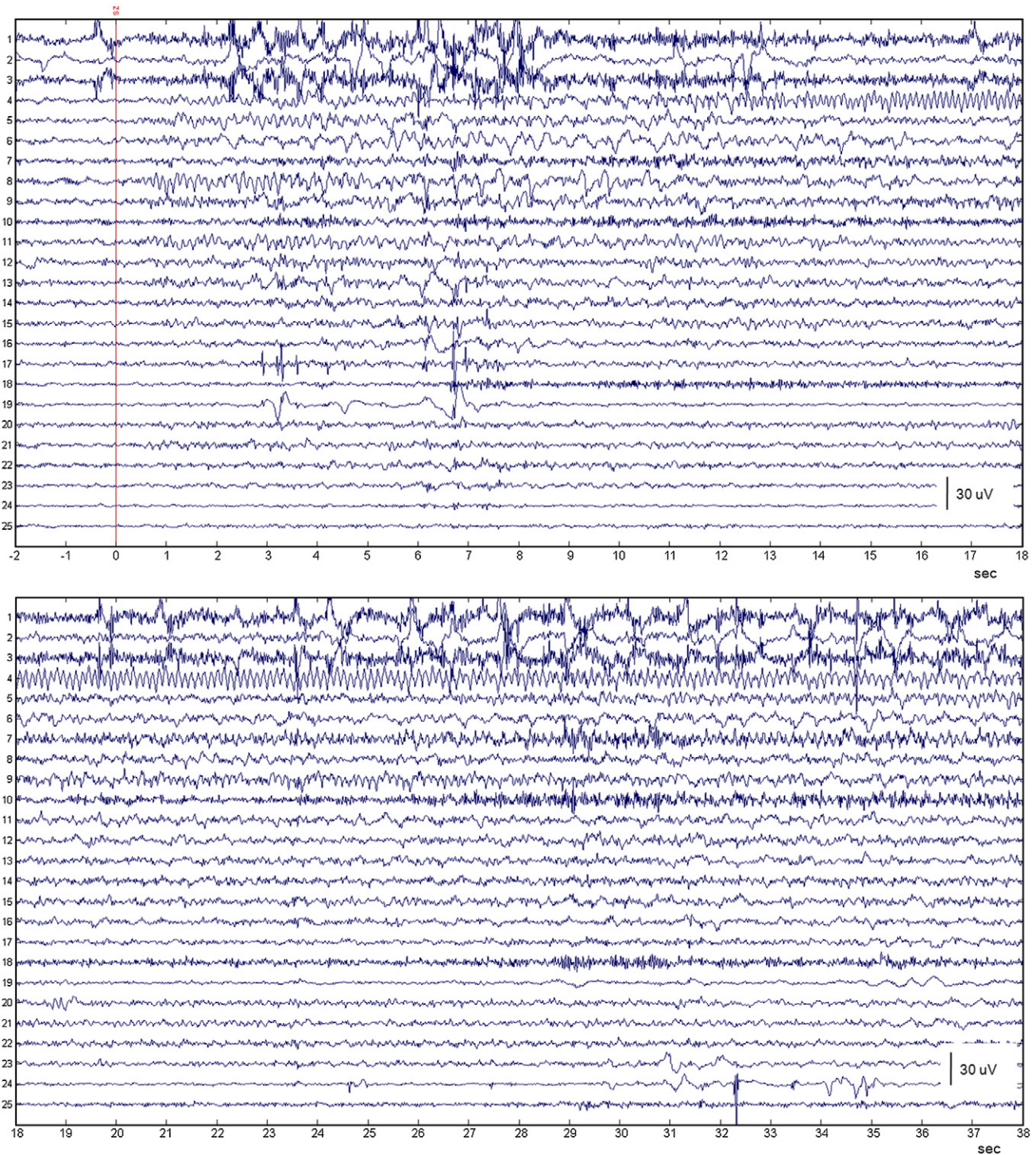


Fig. 2 – ICA decomposition of the seizure described in Fig. 1. Five independent components showed rhythmic activity during seizure progress.

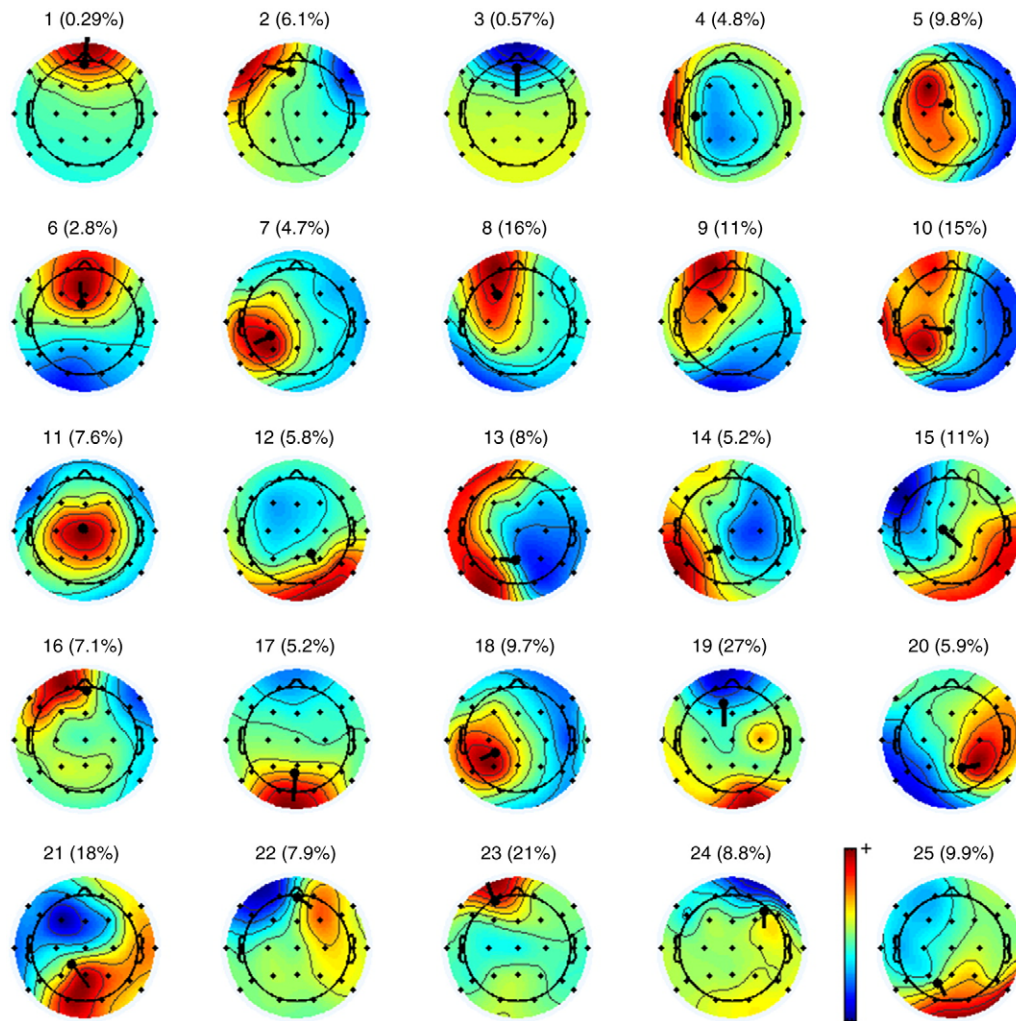


Fig. 3 – Topographic maps of each ICA component for the seizure described in Fig. 1. A single dipole source for each independent component is located on the map. The percentages in parenthesis indicate residual variances of the dipole source.

dipole sources that corresponded to the selected ICs were displayed on a standard MRI template. Event-related spectral perturbation (ERSP) in addition to the time courses of ICs revealed that the activities of lateral temporal, mesial temporal, and inferior frontal regions were dominant in the theta band during the this seizure onset period (Fig. 4). Subsequently, activities of lateral temporal, mesial frontal, and basal ganglia increased. Furthermore, activities due to lateral and mesial temporal sources were followed and found to persist until the end of seizure.

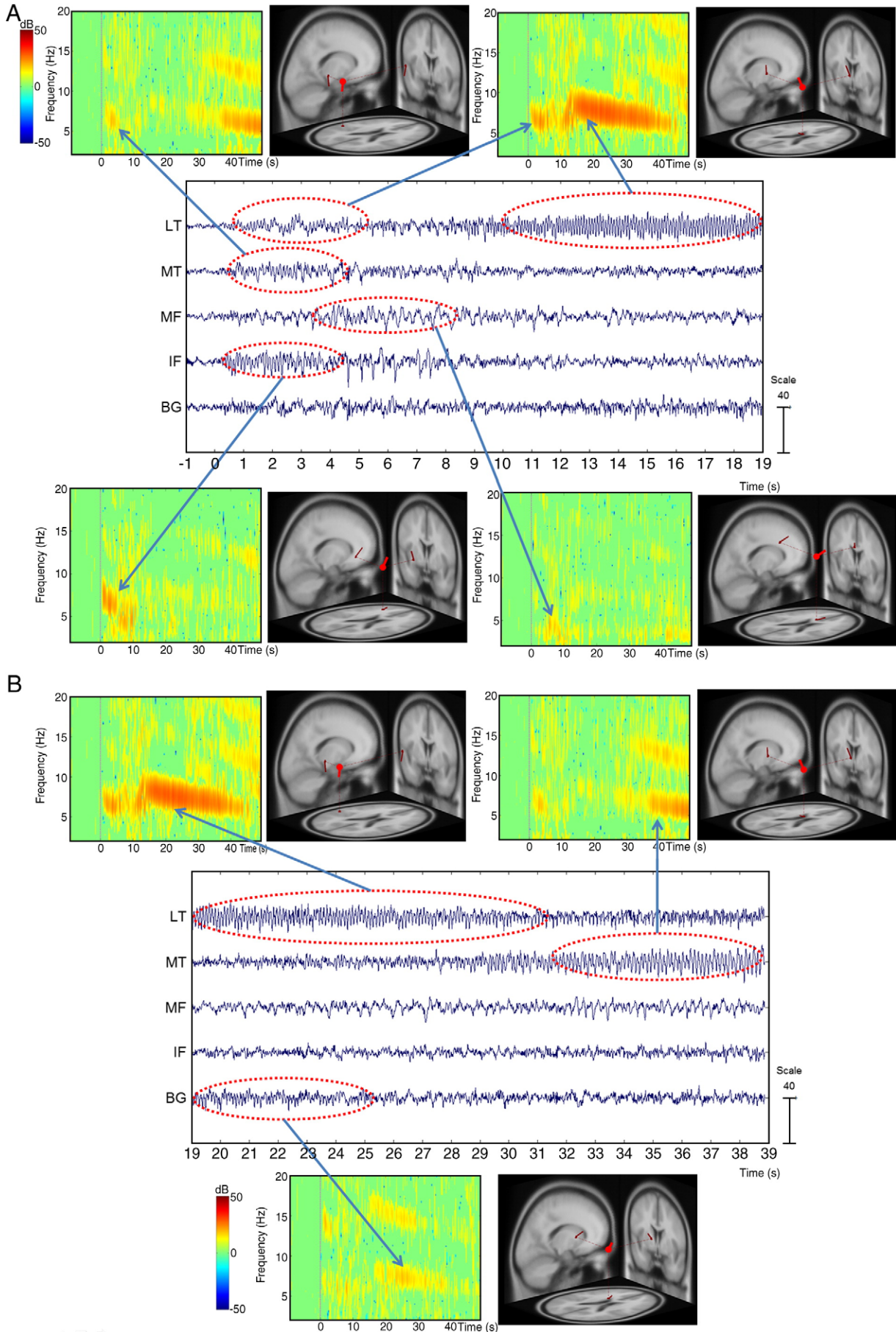
Patient no. 11 was a 40 year old man who had experienced complex partial seizures for 24 years. Brain MRI revealed HS in left temporal lobe, and initial ictal EEG showed bitemporal rhythmic delta activities, which were more dominant in the

left side (Fig. 5). Four ICs were found to be responsible for ictal activities and accounted for 44.8% of total variance during the 30 s following seizure onset. ERSP demonstrated that seizure activity spread from the bilateral mesial temporal to the medial frontal region initially (Fig. 6A), and subsequently spread in the ipsilateral mesial temporal region and basal ganglia, followed by the contralateral mesial temporal region (Fig. 6B).

2.3. Clustering seizure-related ICs across all seizures within-subject (level 2 analysis)

Details of the dipole sources corresponding to all seizures are summarized in Table 2, and the locations of dipole source

Fig. 4 – Time course, event-related spectral perturbations, and dipole source localizations of 5 independent components accounting for rhythmic ictal activity for the seizure described in Fig. 1. (A) During the first half of the seizure, rhythmic activities from the inferior frontal (IF) and lateral temporal (LT) regions were observed. Note that medial temporal (MT) and medial frontal (MF) areas also showed transient, weak rhythmic activity in seizure onset. (B) The activity of basal ganglia (BG) transiently increased during the middle of the seizure, whereas MT activity started to increase prior to seizure cessation. LT regions showed persistently rhythmic activity from 10 s after seizure onset until seizure cessation.



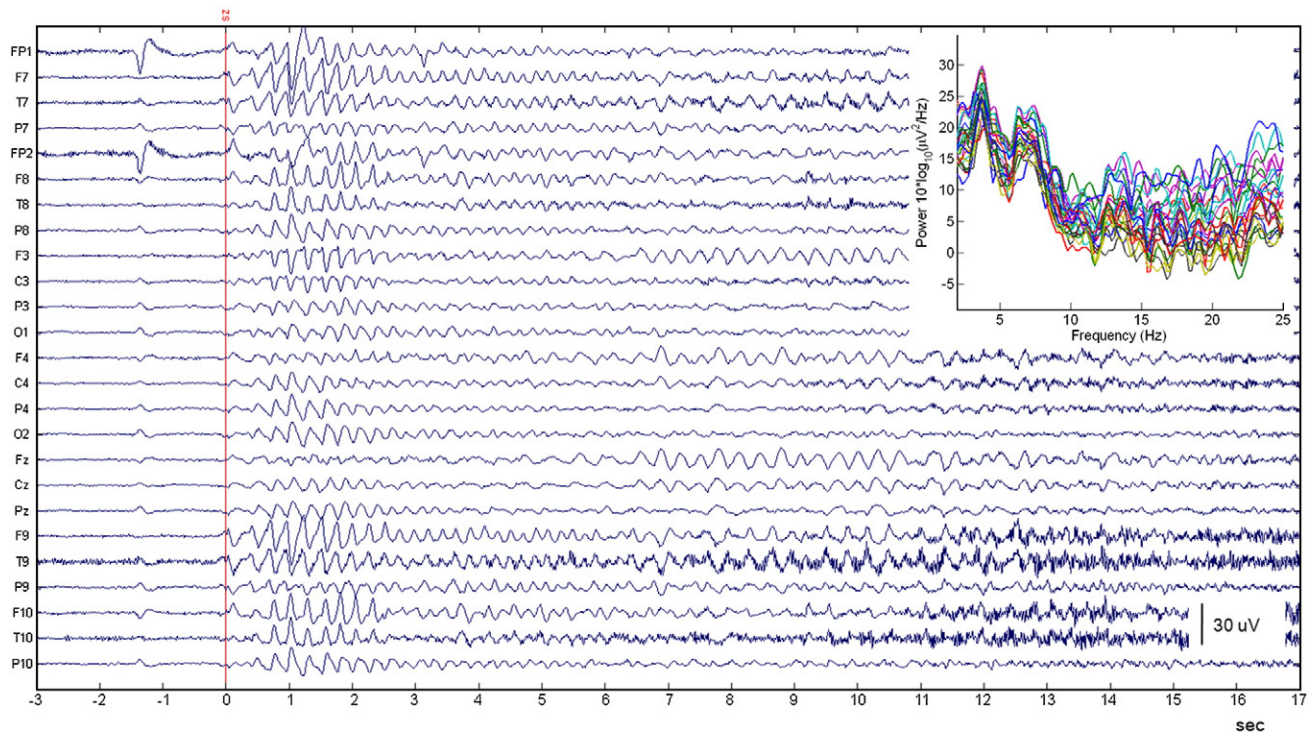


Fig. 5 – An example of a type 2 ictal onset pattern ictal scalp EEG (patient no. 11). The EEG is displayed with common average reference. The red vertical line indicates the onset of EEG seizure. The insert is an overlay of the power spectra of the first 30 s seizure from all channels.

clusters in individual patients are depicted in Fig. 7. From these results, several common characteristics were identified in all patients. Specifically, two to five dipole clusters (mean, 3.2 ± 0.3) were found to be responsible for ictal activities in each patient, and seizures were found to involve mainly the anterior temporal and frontal regions. Furthermore, the mesial and lateral anterior temporal, medial frontal region, and basal ganglia were most commonly involved during temporal lobe seizure progression.

2.4. Clustering dipoles for all seizures and subjects by seizure type (level 3 analysis)

Four dipole source clusters for common ictal activities were identified in all patients of each in each IOP type, as shown in Table 3. We identified distinct propagation patterns for temporal lobe seizures by IOP type, as described below.

2.4.1. Ictal propagation pattern of type 1 seizures

TLE with a type 1 IOP was found to have 4 clusters of ICs that accounted for ictal activities (Figs. 8A–C). ERSF analysis and dipole source localization showed that the spectral power of 5- to 9-Hz rhythmic activity was significantly greater at

seizure onset in the mesial temporal and lateral temporal regions. Elevated spectral power in the temporal region persisted for about 10 s and then diminished, and subsequently, spectral power with a slightly wider frequency range (6–11 Hz) than the initial ictal rhythm increased in medial frontal regions. As seizure evolved, the dominant frequency in medial frontal regions tended to decrease to the delta range, and spectral power diminished at about 40 s. This was followed by rhythmic theta activities of medial frontal and basal ganglia that persisted until seizure cessation.

2.4.2. Ictal propagation pattern of type 2 seizures

The ictal activities of type 2 TLE also consisted of 4 component clusters (Figs. 8D–F). Initial ictal activities of 2–7 Hz arose from the ipsilateral medial temporal region. Although spectral power was not strong, the contralateral medial temporal region showed some transient ictal activity from 5 s after seizure onset. Subsequently, the spectral powers of basal ganglia and of both medial frontal regions increased from 10 s to 15 s. This was followed by strong rhythmic theta to alpha activities of 6–10 Hz in the ipsilateral medial temporal regions, which was accompanied by dipole cluster of basal ganglia. The frequency of rhythmic activities

Fig. 6 – Time course of the event-related spectral perturbations and dipole source localizations of 4 independent components accounting for rhythmic ictal activity for the seizure described in Fig. 5. (A) During the first half of the seizure, rhythmic activities from bilateral mesial temporal regions were observed followed by rhythmic activities from the medial frontal (MF) region. (B) During the second half of the seizure, basal ganglia (BG) and ipsilateral mesial temporal (iMT) activities increased. The contralateral mesial temporal (cMT) region was activated prior to seizure cessation.

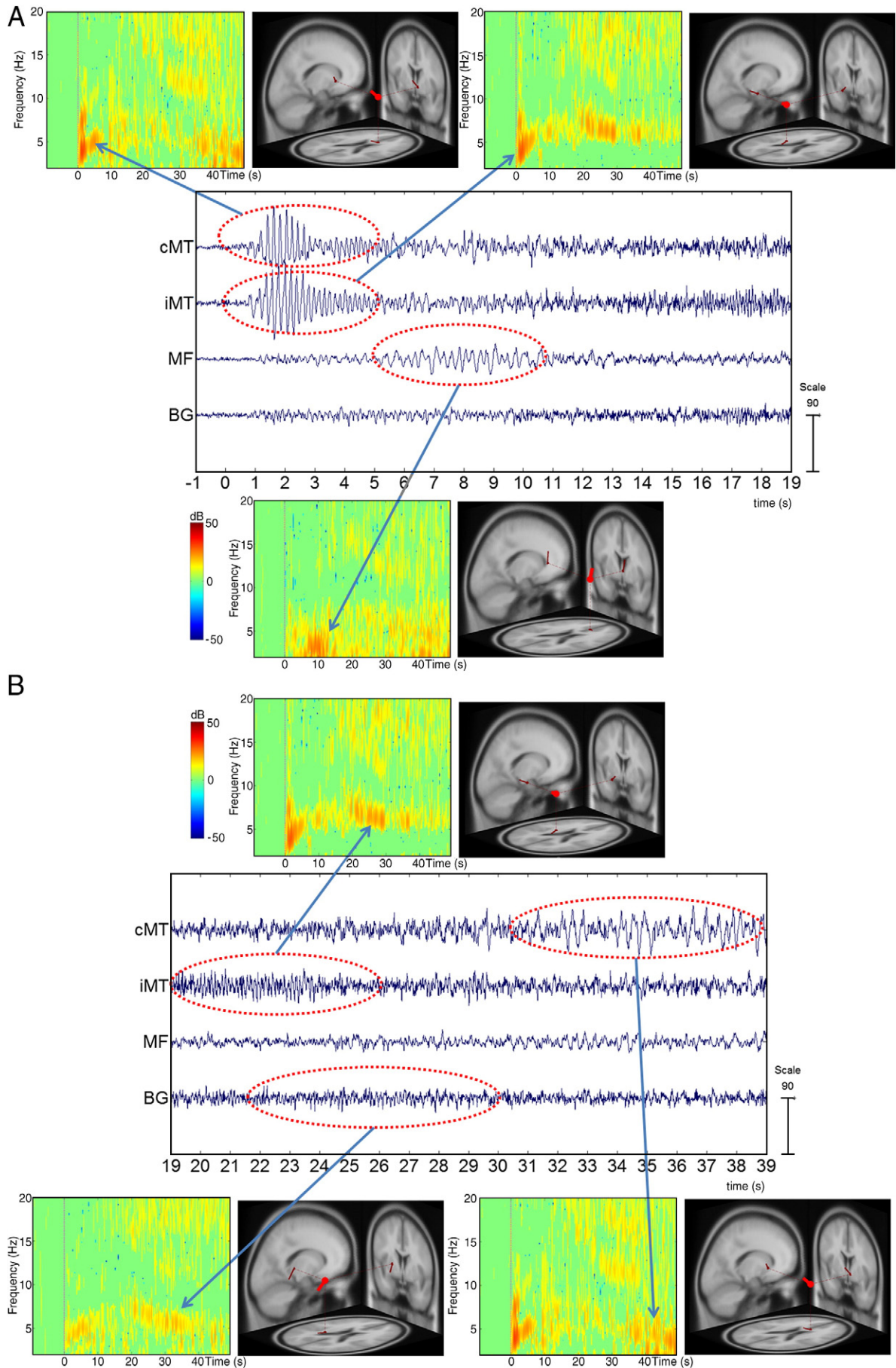


Table 2 – Propagation of dipole sources of all seizures in each patient.

Patient no.	Type	Laterality	No. of seizure	Location of dipole source cluster		
				0–10 s	11–20 s	21–40 s
1	1	L	7	MT, MF	MF	BG, MF
2	1	L	5	MT	MT, BG	BG
3	1	R	2	IF, MT	IF	MF
4	1	R	8	MT	MT, LT	LT, MF
5	2	L	2	AT, MF	AT	BG
6	2	L	3	MF, MT	MT	BG
7	2	R	7	MT, BG	LT, MT, MF	LT, MF
8	2	L	5	MT	MF,	BG, MT, cMT
9	2	R	5	MT	MT, MF, BG	MT, PT
10	2	R	3	MT, LT	MT	MT, MF
11	2	L	5	MT, IF, cMT	BG, DF	MT, BG, DF
12	2	R	2	MF, MT	MT	MF, MT

MT: mesial temporal, LT: lateral temporal, cMT: contralateral mesial temporal, AT: anterior temporal, PT: posterior temporal, MF: medial frontal, IF: inferior frontal, DF: dorsolateral frontal, BG: basal ganglia, L: left, R: right.

decreased progressively to the delta range as seizure progressed.

3. Discussion

Our study suggests that TLE associated with HS has a preferred seizure progression pathway. Initially, we extracted the ictal component by ICA, and then characterized propagation patterns of individual seizures using the spatiotemporal characteristics of dipole sources. It was found that unique seizure propagation patterns were present at the individual and inter-individual levels. Furthermore, group level analysis showed that the ictal propagating patterns was distinct according to the IOP (i.e. type 1 vs. type 2) for temporal lobe seizure.

It has been reported that interictal discharges originate from a complex interaction between separate regions, and that these result in the propagation and recruitment of neuronal activity along specific neural pathways (Alarcon et al., 1994, 1999; Zumsteg et al., 2006). Ictal activity also spreads from the onset zone to other brain regions during seizure progression. Thus, it has been suggested that considerations of ictal propagation patterns and seizure onset zone might enable mesial and neocortical TLE to be differentiated (Bertashius, 1991; Brekelmans et al., 1995; Lieb et al., 1991) and surgical outcome to be predicted in TLE (Schulz et al., 2000). Janszky et al. (2001) demonstrated that contralateral propagation of ictal discharges during temporal lobe seizures can affect the occurrence of interictal epileptiform discharges postictally. These findings indicate that intracerebral propagation should be considered when using non-invasive source algorithms in patients with mesial TLE.

In the present study, we found that ictal discharges associated with type 1 seizures arose from both the anterior temporal region and basal ganglia, and then spread into the medial frontal region. The dominant frequency of ictal rhythm was in the theta range (5–9 Hz) and remained relatively constant until the middle portion of seizures when mixed frequencies in the delta-theta range became predominant. Type 2 seizures of TLE developed in either bilateral or

predominantly ipsilateral mesial temporal region, followed by in the medial frontal region and basal ganglia. Although ictal activities propagated into the lateral temporal region, rhythmic activity predominated in the medial portion of the frontotemporal region. The dominant ictal frequency at seizure onset was in the delta range (2–5 Hz). However, rhythmic theta activities (5–9 Hz) of a decreasing tendency rapidly ensued after seizure onset.

Voltage topography and dipole source localization revealed that initial ictal activities in type 1 seizures occurred in the ipsilateral anterior temporal region, and involved both mesial and lateral areas. On the other hand, in type 2 seizures, the ictal onset zone was either in the unilateral or bilateral (predominantly ipsilateral) deep temporal regions, and gave rise to a diffuse voltage topography. Thereafter, the lateral temporal region became involved. Although the anteromesial temporal, medial frontal, and basal ganglia were commonly involved during temporal lobe seizure, interactions between these regions and propagation patterns were somewhat different for the two IOP types; type 1 seizures showed sequential involvement among these cerebral substrates (anteromesial temporal → basal ganglia → medial frontal region), whereas type 2 seizures showed complex interactions that resulted in the mutual activations of these areas.

ICA-based dipole source localization showed that only a few specific brain regions were responsible for ictal discharges. This finding is in agreement with those of previous studies (Iriarte et al., 2006; Leal et al., 2006). We found that medial frontal region and basal ganglia were commonly involved, regardless of IOP, during temporal lobe seizure. Brekelmans et al. (1995) described three types of ictal spreading patterns using stereo-EEG in mesial TLE. Seizures were found to originate from mesiolimbic structures and to spread to the contralateral mesiolimbic, ipsilateral lateral temporal, or ipsilateral frontal regions, and then to propagate into other regions in these areas (Brekelmans et al., 1995). In a previous stereo-EEG study, Lieb et al. (1991) reported that the most common mode of spread was temporal lobe → ipsilateral frontal lobe → contralateral frontal lobe → contralateral temporal lobe. This finding suggests that the frontal lobe is frequently involved in the propagation of seizures initiated in the mesial temporal lobe. Ictal SPECT

studies, which can reflect whole-brain activity during seizure, demonstrated a specific mesial temporal–frontal–basal ganglia/thalamus network (Kim et al., 2007; Tae et al., 2005). Nevertheless, ictal SPECT provides only in an image of the distribution of cerebral blood flow 1–2 min after tracer administration, resulting in limited temporal resolution with the possibility of imaging secondary spread rather than the site of seizure onset (Duncan, 2002). Accordingly, we regard ictal SPECT as being inappropriate for determining the propagation pathways of ictal discharges. On the other hand, the scalp EEG method used in the present study, has high temporal resolution and provides whole-brain coverage, and it confirmed that there exist specific preferential propagation patterns of ictal activity in TLE.

When we compared the two types of IOPs, no differences were found in terms of MRI findings or clinical features, such as, age of onset, epilepsy duration, history of febrile seizure, frequency of seizure, or surgical outcome. Furthermore, we excluded patients with EEGs showing ictal propagation switching. These findings suggest that the different features of the two IOPs are best attributed to preferential propagation pathways, as was proposed by Ebersole and Pacia (1996). Moreover, because no lesions other than HS were detected by brain MRI and both study groups showed excellent surgical outcomes, the results of the present study suggest that IOP determines the course of propagation in TLE.

Our time-frequency spectral analyses of ictal EEGs showed that the dominant rhythms during the first half of seizure were delta (type 1) or theta to alpha (type 2), which agrees with previous studies. However, ictal discharge frequencies were not constant as seizures progressed, which has not been previously reported. Furthermore, we found that the pattern of frequency change was dependent on IOP type. The dominant theta rhythm of type 1 seizures tended to decrease to the delta range around 10 s after seizure onset. Subsequently, regular rhythmic activities in theta to alpha bands followed and persisted until the mid-part of seizures, and these were followed by irregular rhythmic delta activities of decreasing tendency toward seizure cessation. For type 2 seizures, initial rhythmic delta activities tended to increase rapidly to the theta range within 10–20 s, and then decrease progressively to the delta range at seizure cessation.

The usefulness of ICA in the dipole model and for current density reconstruction has recently been demonstrated for interictal spikes (Barbati et al., 2006; Jung et al., 2005; Kobayashi et al., 2001), event-related potentials (Marco-Pallares et al., 2005), and for ictal EEG data (Iriarte et al., 2006; Leal et al., 2006). Iriarte et al. reported that in focal seizures, including temporal and extratemporal lobe seizures, rhythmic activity can be separated into several components including an initial component that obviously concurs with the focus. In addition, they observed spatiotemporal evolution of ictal components in accord with time of onset of ictal activity in each seizure (Iriarte et al., 2006). Leal et al. (2006) demonstrated rhythmic ictal activity in a single dataset merged from multiple seizures by ICA decomposition. They found common spreading patterns of gelastic seizures was associated with early, brief epileptic generators in deep subcortical regions and later activations of more superficial generators. However, neither study evaluated common ictal propagation patterns at

the group level in a given epilepsy syndrome. Thus, to the best of our knowledge, this is the first study to explore common propagation patterns in a homogeneous epilepsy syndrome.

The present study has several limitations. For some seizures, ICA could not clearly separate ictal EEG into temporally independent components, which resulted in considerable overlap between components. This could be attributed to several factors, such as, the smearing effect of the skull, a limited number of electrodes, and unavoidable intermixed artifacts. Furthermore, because we identified propagation according to time of onset of the ictal activity by visual inspection, functional connectivities and information flows between ICs were not taken into consideration. In addition, averaging across components clustered solely based on equivalent dipole location hinders determinations of the exact spread of seizure activity. Further study is required to overcome these limitations.

In conclusion, our findings suggest that mesial temporal lobe seizures associated with HS have specific propagation patterns that are ictal onset pattern dependent. Furthermore, our findings indicate that ICA-based ictal source localization could be used to identify ictal propagation patterns and ictal onset zones.

4. Experimental procedures

4.1. Patients

Pre-surgical EEG data from 12 patients that had undergone temporal lobectomy for medically intractable epilepsy were analyzed. All patients had; (a) electroclinical features typical of TLE during pre-surgical long-term video-EEG monitoring; (b) unilateral HS by high-resolution MRI; (c) undergone anterior temporal lobectomy and amygdalohippocampotomy with a minimum follow-up of 2 years; (d) a surgical pathology demonstrating HS without dual pathology; and (e) an excellent surgical outcome (Engel class I). HS was diagnosed by visually assessing high-resolution MR images, based on the presence of unilateral hippocampal atrophy and an increased T2 signal in the atrophic hippocampus (Jackson et al., 1993). Patients that exhibited both type 1 and 2 IOP were excluded. Patients with the following EEG features were also excluded: (a) non-lateralizing ictal scalp EEG, such as, generalized delta-to-theta or a slow or diffuse electrodecremental pattern within 10 s of seizure onset; and (b) switching of lateralized ictal discharges to the contralateral side during seizure evolution.

4.2. Acquisition, selection, and classification of ictal scalp EEG findings

Ictal scalp EEGs were acquired using a 64-channel digital video-EEG system (Vanguard system; Cleveland, OH) for pre-surgical evaluations. Forty to 48 scalp electrodes were placed according to the International 10–10 System, with supplementary subtemporal and sphenoidal electrodes. The band pass filter was set at 0.5–70.0 Hz with a sampling rate of 200 Hz. Ictal EEG onset was defined as the presence of well-recognized, sustained rhythmic activities that were evident from the background. Two types of lateralizing IOPs were

identified as utilized by the Ebersole and Pacia classification (Ebersole and Pacia, 1996), namely; (a) those with a sustained regular 5- to 9-Hz rhythm with a well-lateralized temporal or

subtemporal distribution (type 1); and (b) those with an irregular 2- to 5-Hz rhythm with a widely spread temporal distribution (type 2).

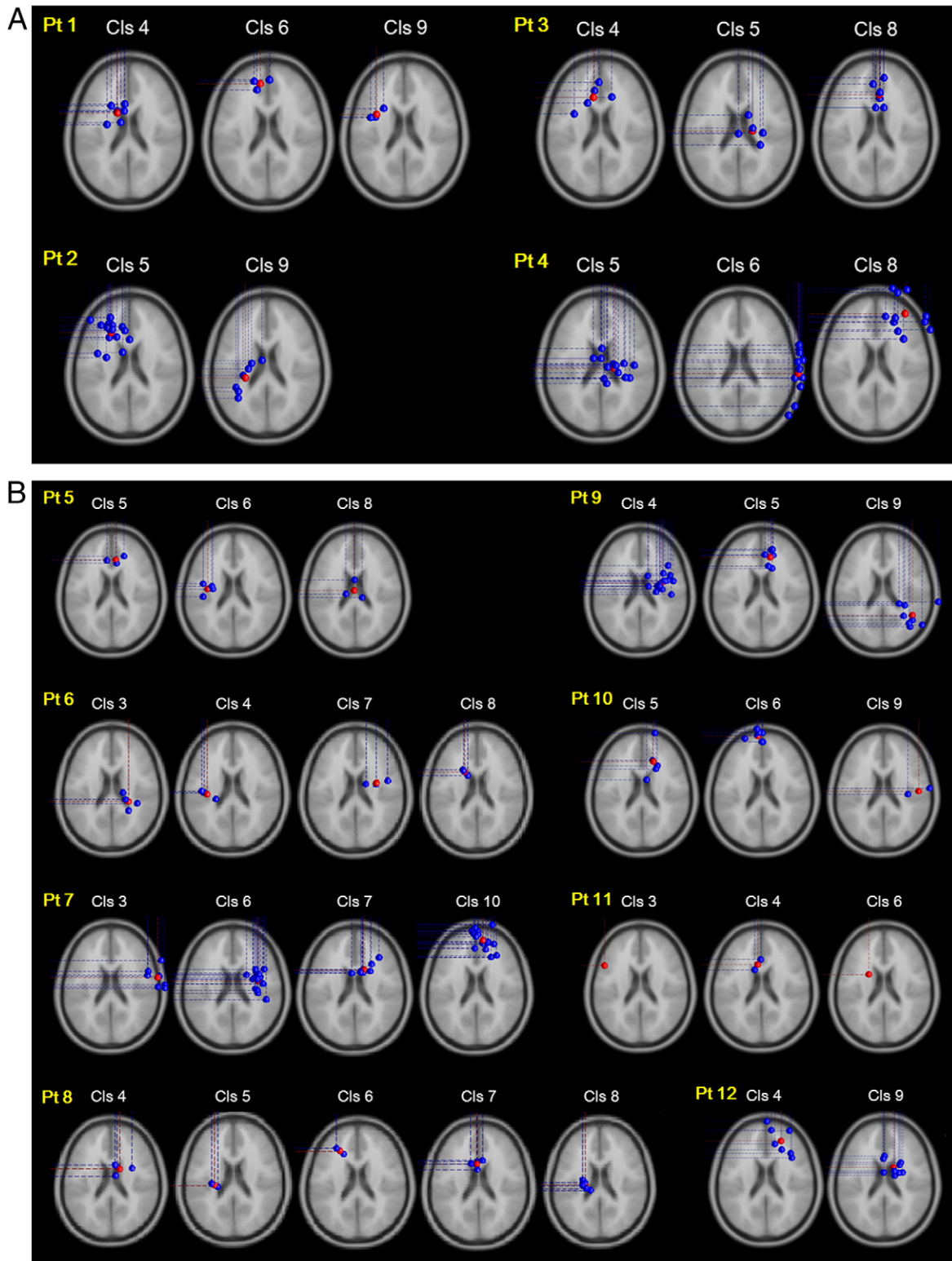


Fig. 7 – Cluster analysis of all seizures revealed the locations of dipole source clusters in patients. (A) type 1 seizure and (B) type 2 seizure. Blue dots indicate the independent components, and red dots indicate the centroid of clustered components in given clusters.

Table 3 – Common pattern of ictal propagation in each group.

	Type 1	Type 2
No. of seizures analyzed	22	33
Mean no. of IC per seizure	3.1	3.0
No. of dipole clusters within group	4	4
Location of dipole source cluster		
0–10 s	MT, LT	iMT, cMT
11–20 s	MF	BG, MF
21–40 s	MT, BG	iMT, BG

IC: independent component, iMT: ipsilateral medial temporal, cMT: contralateral medial temporal, MF: medial frontal, BG: basal ganglia, Cls: dipole source cluster.

4.3. Independent component analysis of ictal EEG data

As most seizures had durations of around 60 s (Table 1), EEG data were analyzed from –10 s to +50 s with respect to seizure onset. For analysis purposes, we selected equally distributed 25 electrodes (Fp1, F7, T7, P7, F3, C3, P3, O1, Fp2, F8, T8, P8, F4, C4, P4, O2, Fz, Cz, Pz, F9, T9, P9, F10, T10, and P10). EEGs were re-referenced against a common average reference and filtered at frequencies of 1.0–30 Hz. The EEG data matrix was then decomposed using ICA-based on a simple neural network algorithm that could blindly separate mixtures of independent sources using information maximization (Bell and Sejnowski, 1995). The open source ICA program EEGLAB version 6.01 (Delorme and Makeig, 2004) was used in the MATLAB environment (version 7.01; MathWorks, Natick, MA).

4.4. Dipole source localization of ictal components

To identify the source locations of ICs responsible for ictal activities, we used a single equivalent dipole source model, and the DIPFIT function in EEGLAB, which utilizes the non-linear fitting of a single dipole model, to explain scalp potential distributions (Scherg, 1990). Source location was estimated within a four-shell, spherical model of the head. For the head model, we assumed conductivities (mhos/m) of 0.33, 0.0042, 1.00, and 0.33 for the scalp, skull, CSF, and brain, respectively. The radii of the spheres were standardized at 85, 79, 72, and 71 mm, respectively. Transposition of dipole location from the spherical head model to the average MRI template was accomplished using DIPFIT, by co-registering electrode landmark positions and the Montreal Neurological Institute average brain image.

4.5. Selection of relevant ictal components

The ICA algorithm produced 25 ICs. The ICs that accounted for ictal activity were selected using previously described procedures (Iriarte et al., 2006; Leal et al., 2006; Onton et al., 2005). Initially, decomposed IC activations were plotted temporally and mapped spatially to scalp topography. ICs of extracerebral origin, including muscle artifacts, eye movements, and 60-Hz noise, were excluded by visually inspecting scalp voltage topography and activation spectra. After localizing a single dipole source for each IC using DIPFIT, ICs of dipole sources

located outside the head model or with a residual variance of more than 20% were excluded. Of the remaining ICs, only those clearly found to contain ictal activity were included (Iriarte et al., 2006).

4.6. Clustering of dipole sources across seizures

To identify common patterns of ictal propagation across seizures in individual patients or in a given group, we defined multiple clusters that represented relatively common EEG activities across seizures. Closely located dipole sources were classified into same subsets (clusters), according to distances measured in vector space using the K-means algorithm, in EEGLAB (Jung et al., 2007; Onton et al., 2005; Onton et al., 2006). This algorithm clusters objects into k partitions based on attributes (MacQueen, 1967). The algorithm starts by partitioning input points into k initial sets and then assigns observations to clusters so as to minimize the total within-class sums of squares. We set 7 as the initial k value and 3 SD as the outlier cut-off. After inspection of initial clustering results, the k value was adjusted stepwise until the resulting clusters were stable and anatomically plausible.

4.7. Time frequency spectral analysis: event-related spectral perturbation

To identify sequences of propagation among multiple components or among component clusters during seizures, seizure-related spectral power changes (in dB) were analyzed using event-related spectral perturbation (ERSP) indices (Makeig, 1993), defined as;

$$\text{ERSP}(f, t) = \Sigma |F_k(f, t)|^2 \quad (1)$$

where, $F_k(f, t)$ is the spectral estimate of seizure k at frequency f and time t . ERSP are mean time-frequency points across seizures, where higher or lower spectral power differs from mean power during the 10 s pre-ictal baseline period. To determine the threshold significance of ERSP, we used bootstrap distributions ($P < 0.01$), extracted randomly from baseline data (10 s before seizure onset) and applied 200 times (Makeig et al., 2002). The color of image pixels indicated changes in power (in dB) at given frequencies, and latency relative to baseline. Based on the ERSP profiles of ICs, ictal propagation across ICs was identified at three arbitrarily predefined periods (0–10 s, 11–20 s, and 21–40 s) according to the time of ictal activity onset in the ERSP plot (Iriarte et al., 2006; Leal et al., 2006).

4.8. Stepwise analyses of clustering ICs

We analyzed data at three levels. Seizures were separately decomposed by ICA, and the sources of ICs were uniquely localized for each seizure. During level 1 analysis, we examined seizure propagation patterns for each seizure event. During level 2 analysis clustered, we examined seizure-related ICs for individual patients. This approach is important for clinically applications that require confirmation of ictal patterns in patients with for intractable epilepsy scheduled for surgery. Finally, level 3 analysis involved clustering dipoles across all seizures, for all subjects, by seizure type (i.e., Types 1 and 2).

Because numbers of seizures, seizure-related ICs, and seizure propagation patterns were no different for left and

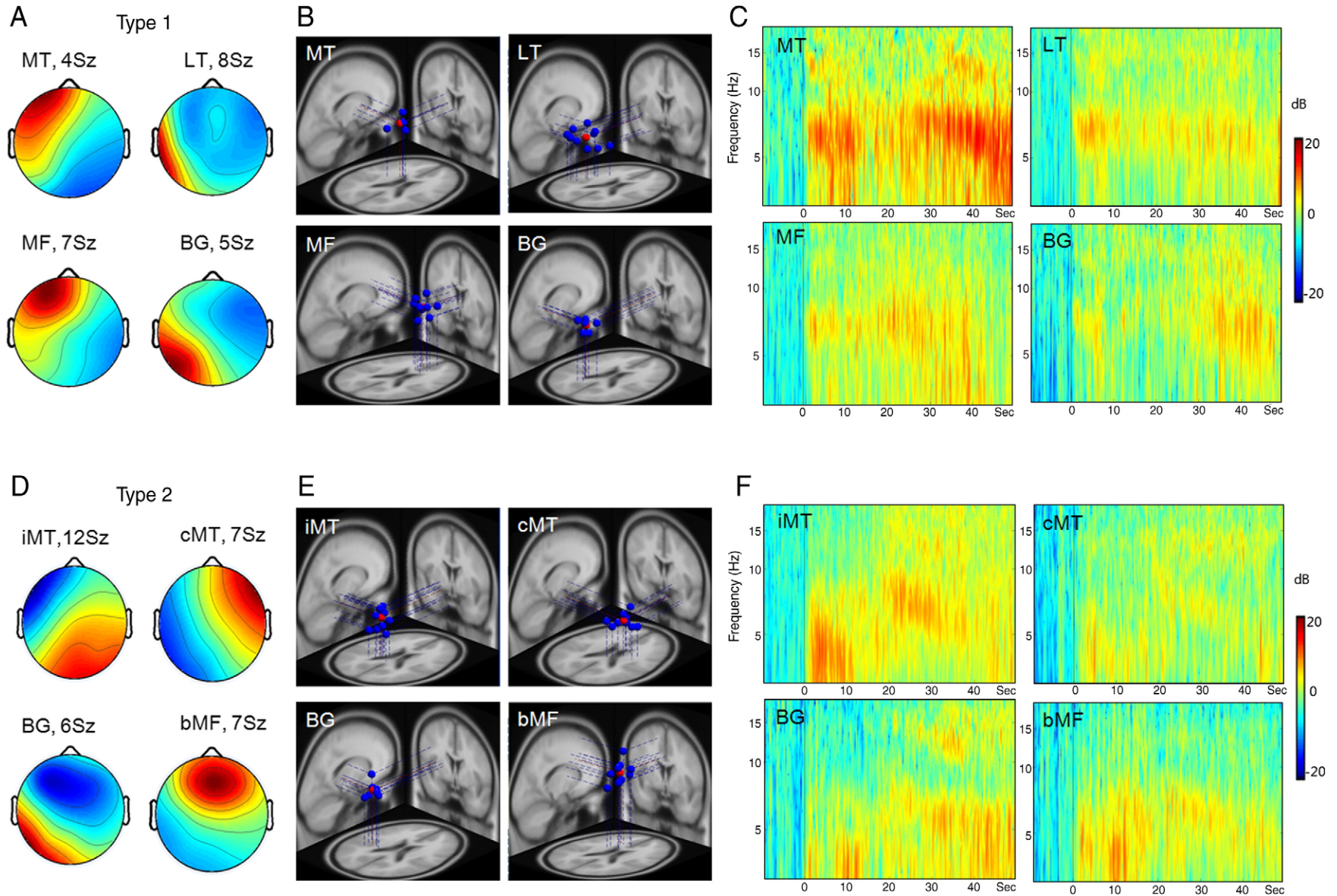


Fig. 8 – Cluster analysis showed four distinct clusters of dipole sources in each seizure type. Top: type 1, Bottom: type 2, (A, D) Mean voltage topography, (B, E) Location of dipole clusters on standard MRI templates, (C, F) mean event-related spectral perturbation. Cls: numeric of dipole cluster, Sz: number of seizures involved in the same cluster, MT: mesial temporal, LT: lateral temporal, iMT: ipsilateral mesial temporal, cMT: contralateral mesial temporal, MF: medial frontal, bMF: bilateral medial frontal, BG: basal ganglia.

right TLE patients, the EEG data matrices of right TLE patients were reflected about midline to allow group comparisons.

Acknowledgments

This work was supported by the Korea Science and Engineering Foundation (KOSEF) grant funded by the Korea government (MEST) (no. 2009-0073377) and grant from Korea University (K0714531). Drs. Jung and Kang contributed equally as co-first authors in this study.

Appendix A. Supplementary data

Supplementary data associated with this article can be found, in the online version, at [doi:10.1016/j.brainres.2009.06.071](https://doi.org/10.1016/j.brainres.2009.06.071).

REFERENCES

- Alarcon, G., Guy, C.N., Binnie, C.D., Walker, S.R., Elwes, R.D., Polkey, C.E., 1994. Intracerebral propagation of interictal activity in partial epilepsy: implications for source localisation. *J. Neurol. Neurosurg. Psychiatry* 57, 435–449.
- Alarcon, G., Binnie, C.D., Garcia Seoane, J.J., Martin Miguel, M.C., Fernandez Torre, J.L., Polkey, C.E., Guy, C.N., 1999. Mechanisms involved in the propagation of interictal epileptiform discharges in partial epilepsy. *Electroencephalogr. Clin. Neurophysiol. Suppl.* 50, 259–278.
- Barbati, G., Sigismondi, R., Zappasodi, F., Porcaro, C., Graziadio, S., Valente, G., Balsi, M., Rossini, P.M., Tecchio, F., 2006. Functional source separation from magnetoencephalographic signals. *Hum. Brain. Mapp.* 27, 925–934.
- Bell, A.J., Sejnowski, T.J., 1995. An information-maximization approach to blind separation and blind deconvolution. *Neural. Comput.* 7, 1129–1159.
- Bertshius, K.M., 1991. Propagation of human complex-partial seizures: a correlation analysis. *Electroencephalogr. Clin. Neurophysiol.* 78, 333–340.
- Brekelmans, G.J., van Emde Boas, W., Velis, D.N., van Huffelen, A.C., Chr. Debets, R.M., van Veelen, C.W., 1995. Mesial temporal versus neocortical temporal lobe seizures: demonstration of different electroencephalographic spreading patterns by combined use of subdural and intracerebral electrodes. *J. Epilepsy* 8, 309–320.
- Delorme, A., Makeig, S., 2004. EEGLAB: an open source toolbox for analysis of single-trial EEG dynamics including independent component analysis. *J. Neurosci. Methods* 134, 9–21.
- Duncan, J.S., 2002. Neuroimaging methods to evaluate the etiology and consequences of epilepsy. *Epilepsy Res.* 50, 131–140.
- Ebersole, J.S., Pacia, S.V., 1996. Localization of temporal lobe foci by ictal EEG patterns. *Epilepsia* 37, 386–399.
- Ebner, A., Hoppe, M., 1995. Noninvasive electroencephalography and mesial temporal sclerosis. *J. Clin. Neurophysiol.* 12, 23–31.
- Iriarte, J., Urrestarazu, E., Artieda, J., Valencia, M., Levan, P., Viteri, C., Alegre, M., 2006. Independent component analysis in the study of focal seizures. *J. Clin. Neurophysiol.* 23, 551–558.
- Jackson, G.D., Berkovic, S.F., Duncan, J.S., Connelly, A., 1993. Optimizing the diagnosis of hippocampal sclerosis using MR imaging. *AJNR Am. J. Neuroradiol.* 14, 753–762.
- Janszky, J., Fogarasi, A., Jokeit, H., Schulz, R., Hoppe, M., Ebner, A., 2001. Spatiotemporal relationship between seizure activity and interictal spikes in temporal lobe epilepsy. *Epilepsy Res.* 47, 179–188.
- Jung, K.Y., Kim, J.M., Kim, D.W., Chung, C.S., 2005. Independent component analysis of generalized spike-and-wave discharges: primary versus secondary bilateral synchrony. *Clin. Neurophysiol.* 116, 913–919.
- Jung, K.Y., Seo, D.W., Na, D.L., Chung, C.S., Lee, I.K., Oh, K., Im, C.H., Jung, H.K., 2007. Source localization of periodic sharp wave complexes using independent component analysis in sporadic Creutzfeldt-Jakob disease. *Brain Res.* 1143, 228–237.
- Kim, J.H., Im, K.C., Kim, J.S., Lee, S.A., Lee, J.K., Khang, S.K., Kang, J.K., 2007. Ictal hyperperfusion patterns in relation to ictal scalp EEG patterns in patients with unilateral hippocampal sclerosis: a SPECT study. *Epilepsia* 48, 270–277.
- Kobayashi, K., Merlet, I., Gotman, J., 2001. Separation of spikes from background by independent component analysis with dipole modeling and comparison to intracranial recording. *Clin. Neurophysiol.* 112, 405–413.
- Lantz, G., Grave de Peralta Menendez, R., Gonzalez Andino, S., Michel, C.M., 2001. Noninvasive localization of electromagnetic epileptic activity. II. Demonstration of sublobar accuracy in patients with simultaneous surface and depth recordings. *Brain Topogr.* 14, 139–147.
- Leal, A.J., Dias, A.I., Vieira, J.P., 2006. Analysis of the EEG dynamics of epileptic activity in gelastic seizures using decomposition in independent components. *Clin. Neurophysiol.* 117, 1595–1601.
- Lieb, J.P., Dasheiff, R.M., Engel Jr, J., 1991. Role of the frontal lobes in the propagation of mesial temporal lobe seizures. *Epilepsia* 32, 822–837.
- MacQueen, J.B., 1967. Some Methods for classification and analysis of multivariate observations. *Proceedings of 5-th Berkeley Symposium on Mathematical Statistics and Probability. University of California Press, Berkeley*, pp. 281–297.
- Makeig, S., 1993. Auditory event-related dynamics of the EEG spectrum and effects of exposure to tones. *Electroencephalogr. Clin. Neurophysiol.* 86, 283–293.
- Makeig, S., Westerfield, M., Jung, T.P., Enghoff, S., Townsend, J., Courchesne, E., Sejnowski, T.J., 2002. Dynamic brain sources of visual evoked responses. *Science* 295, 690–694.
- Marco-Pallares, J., Grau, C., Ruffini, G., 2005. Combined ICA-LORETA analysis of mismatch negativity. *NeuroImage* 25, 471–477.
- Nam, H., Yim, T.G., Han, S.K., Oh, J.B., Lee, S.K., 2002. Independent component analysis of ictal EEG in medial temporal lobe epilepsy. *Epilepsia* 43, 160–164.
- Onton, J., Delorme, A., Makeig, S., 2005. Frontal midline EEG dynamics during working memory. *NeuroImage* 27, 341–356.
- Onton, J., Westerfield, M., Townsend, J., Makeig, S., 2006. Imaging human EEG dynamics using independent component analysis. *Neurosci. Biobehav. Rev.* 30, 808–822.
- Pacia, S.V., Ebersole, J.S., 1997. Intracranial EEG substrates of scalp ictal patterns from temporal lobe foci. *Epilepsia* 38, 642–654.
- Scherg, M., 1990. Fundamentals of dipole source potential analysis. In: Grandori, F., Hoke, M., Romani, G. (Eds.), *Auditory Evoked Magnetic Fields and Electric Potentials. Vol. Advances in Audiology. Karger, Basel*, pp. 40–69.
- Schulz, R., Luders, H.O., Hoppe, M., Tuxhorn, I., May, T., Ebner, A., 2000. Interictal EEG and ictal scalp EEG propagation are highly predictive of surgical outcome in mesial temporal lobe epilepsy. *Epilepsia* 41, 564–570.
- Tae, W.S., Joo, E.Y., Kim, J.H., Han, S.J., Suh, Y.L., Kim, B.T., Hong, S.C., Hong, S.B., 2005. Cerebral perfusion changes in mesial temporal lobe epilepsy: SPM analysis of ictal and interictal SPECT. *NeuroImage* 24, 101–110.
- Tao, J.X., Baldwin, M., Ray, A., Hawes-Ebersole, S., Ebersole, J.S., 2007. The impact of cerebral source area and synchrony on recording scalp electroencephalography ictal patterns. *Epilepsia* 48, 2167–2176.
- Zumsteg, D., Friedman, A., Wieser, H.G., Wennberg, R.A., 2006. Propagation of interictal discharges in temporal lobe epilepsy: correlation of spatiotemporal mapping with intracranial foramen ovale electrode recordings. *Clin. Neurophysiol.* 117, 2615–2626.